

Lateral Membrane Biogenesis in Human Bronchial Epithelial Cells Requires 190-kDa Ankyrin-G*[§]

Received for publication, December 30, 2003, and in revised form, January 26, 2004
Published, JBC Papers in Press, February 1, 2004, DOI 10.1074/jbc.M314296200

Krishnakumar Kizhatil† and Vann Bennett

From the Howard Hughes Medical Institute and Departments of Cell Biology, Biochemistry, and Neuroscience, Duke University Medical Center, Durham, North Carolina 27710

Ankyrin-G polypeptides are required for restriction of voltage-gated sodium channels, L1 cell adhesion molecules, and β IV spectrin to axon initial segments and are believed to couple the Na/K-ATPase to the spectrin-actin network at the lateral membrane in epithelial cells. We report here that depletion of 190-kDa ankyrin-G in human bronchial epithelial cells by small interfering RNA results in nearly complete loss of lateral plasma membrane in interphase cells, and also blocks *de novo* lateral membrane biogenesis following mitosis. Loss of the lateral membrane domain is accompanied by an expansion of apical and basal plasma membranes and preservation of apical-basal polarity. Expression of rat 190-kDa ankyrin-G, which is resistant to human small interfering RNA, prevents loss of the lateral membrane following depletion of human 190-kDa ankyrin-G. Human 220-kDa ankyrin-B, a closely related ankyrin isoform, is incapable of preserving the lateral membrane following 190-kDa ankyrin-G depletion. Moreover, analysis of rat 190-kDa ankyrin G/ankyrin B chimeras shows that all three domains of 190-kDa ankyrin-G are required for preservation of the lateral membrane. These results demonstrate that 190-kDa ankyrin-G plays a pleiotropic role in assembly of lateral membranes of bronchial epithelial cells.

Assembly of specialized plasma membrane domains is a fundamental aspect of morphogenesis and physiological function of metazoan tissues (1, 2). Specification of the composition of membrane domains involves a combination of selective retention, *de novo* assembly from presorted membrane components, as well as remodeling through endocytosis-based sorting. The relative balance between these processes apparently varies extensively between epithelial cell types, and even within different epithelial cell lines (2). A current challenge is to define the underlying common mechanisms for formation of membrane domains that may be shared by cells as diverse as neurons and epithelial tissues. The recent discovery of conserved proteins required for polarity in cells ranging from *Caenorhabditis elegans* single-cell zygotes to mammalian epithelial cells (3–5) provides confidence that conserved pathways also exist for configuring plasma membrane domains.

Ankyrins are a family of adaptor proteins present in most

metazoan cells that associate with a diverse group of integral membrane proteins localized in specialized membrane domains (6). One example of polarized ankyrin-binding proteins are voltage-gated sodium channels and L1 cell adhesion molecules, which colocalize with 270/480-kDa ankyrin-G in axonal initial segments and nodes of Ranvier (7–9). Another instance is the Na/K-ATPase,¹ which localizes with 190-kDa ankyrin-G in basolateral domains of epithelial tissues (10–12).

Targeted disruption of ankyrin-G in the mouse cerebellum results in the loss of 270/480-kDa ankyrin-G at Purkinje neuron axon initial segment accompanied by severe ataxia, loss of ability to fire action potentials, and loss of restricted localization of the voltage-gated sodium channel Nav1.6, L1 cell adhesion molecules neurofascin and NrCAM, and β IV spectrin (9). These observations indicate that 270/480-kDa ankyrin-G is required for recruitment of multiple proteins to axon initial segments and may play a role in assembly of this domain.

Ankyrin-G in epithelial cells has been proposed to retain the Na/K-ATPase within the lateral membrane domain by coupling to the spectrin-based membrane skeleton (13). The sequence of events in assembly of the Na/K-ATPase in the lateral membrane has been suggested to begin with cell-cell adhesion mediated by E-cadherin (13, 14). Spectrin is then believed to be recruited to the sites of cell-cell adhesion through an interaction of α -catenin that binds to E-cadherin through β -catenin (15). The Na/K-ATPase, according to this model, is retained at the lateral membrane by binding ankyrin that tethers it to the spectrin-based membrane skeleton (13). A complex containing E-cadherin, spectrin, and ankyrin has been immunoprecipitated from polarized MDCK epithelial cells (16). Moreover, expression of the actin-binding domain of β -2-spectrin blocks assembly of the Na/K-ATPase (17).

Several considerations suggest that spectrin may not be the primary membrane linker for ankyrin in epithelial tissues *in vivo*. Depletion of the sole α - and β -spectrin in *C. elegans* by RNAi (18) or by null mutation (19, 20) revealed that spectrin, although essential for embryonic elongation and survival, was not required for the morphogenesis of polarized epithelial cells. Another caveat is that expression of β -2-spectrin domains can cause cell death (21). Moreover, spectrin reversibly dissociates from sites at cell-cell contact under certain experimental conditions, whereas ankyrin remains membrane-associated (22).

The role of ankyrin-G in epithelial cells has not been experimentally tested. The single *C. elegans* ankyrin gene, *unc-44*, produces multiple transcripts, and the lone *unc-44* allele removes a single transcript that displays an axon guidance defect

* The costs of publication of this article were defrayed in part by the payment of page charges. This article must therefore be hereby marked "advertisement" in accordance with 18 U.S.C. Section 1734 solely to indicate this fact.

[§] The on-line version of this article (available at <http://www.jbc.org>) contains supplementary Fig. 1.

† To whom correspondence should be addressed: Box 3892, Duke University Medical Center, Durham, NC 27710. Tel.: 919-684-4343/684-3538; Fax: 919-684-3590; E-mail: k.kizhatil@cellbio.duke.edu.

¹ The abbreviations used are: Na/K-ATPase, sodium-potassium ATPase; nt, nucleotide; GFP, green fluorescent protein; PBS, phosphate-buffered saline; FITC, fluorescein isothiocyanate; TRITC, tetramethylrhodamine isothiocyanate; MDCK, Madin-Darby canine kidney; siRNA, small interfering RNA.

(23, 24). We have used small interfering RNA (siRNA) encoded by a plasmid (25) to knock down the transcript encoding 190-kDa ankyrin-G in a polarized human bronchial epithelial cell line. This study reveals that ankyrin-G is required for lateral membrane biogenesis and preservation of the lateral membrane at steady state.

EXPERIMENTAL PROCEDURES

Plasmids and Cloning—The pSuper plasmid (25) was a gift from Dr. R. Agami (Netherlands Cancer Institute). 64-nt oligonucleotides were annealed and cloned as described into the pSuper plasmid (25). 19-nt siRNA target regions in the human ankyrin-G (GenBankTM NM_020987) membrane binding domain were chosen based on two criteria. 1) Nucleotide sequences were unique to the membrane-binding domain of the 190-kDa epithelial isoforms of ankyrin-G. 2) The nucleotide sequences were flanked 5' by AA and on the 3' by TT (25). 190-kDa ankyrin-G protein levels were depleted when the 19-nt ankyrin-G sequence, 5'-CATTTCGAATCAGAATGGG-3', was targeted by the siRNA. The plasmids encoding rat 190-kDa ankyrin-G fused at the C terminus to GFP, human 220-kDa ankyrin-B fused at the C terminus to GFP, and chimeras between 190-kDa ankyrin-G and 220-kDa ankyrin-B have been described (26).

Antibodies—Anti-C-terminal ankyrin-G antibody was raised in rabbits following immunization with a recombinant protein composed of the death domain and regulatory C terminus of ankyrin-G. Antibody was purified on an affinity column made with the antigen. Anti-GFP antibody was made by immunization of a pig with purified recombinant GFP protein. The antibody was purified on a GFP affinity column. The affinity-purified β -2-spectrin antibody directed against spectrin repeats 4–9 has been described before (21).

Cell Line and Transfection—Human bronchial epithelial cells were a gift of Dr. Peter Mohler. The cells were grown in Dulbecco's modified Eagle's medium (Invitrogen) supplemented with 10% fetal bovine serum (Sigma). Cells were trypsinized, and 60,000 cells were plated on 1.4-mm coverslip inserts of Matek plates (300 cells/mm²). Cells were transfected using LipofectAMINE 2000 (Invitrogen) after 12 h with 1 μ g of siRNA plasmid. For rescue experiments 100 ng of the rescue plasmid were mixed with 1 μ g of siRNA plasmid and then transfected using LipofectAMINE 2000. The cells were analyzed at 14, 18, and 24 h post-transfection for cell survival using trypan blue dye exclusion. For immunoblot analysis 60-mm dishes were seeded with cells at 300 cells/mm² and transfected with 5 μ g of siRNA plasmid after 12 h. 14 h after transfection cells were lysed and processed for SDS-PAGE.

Immunofluorescence—Cells were fixed using 1% paraformaldehyde for 15 min. The cells were then permeabilized with 0.1% Triton X-100 in 0.25% paraformaldehyde/PBS. Cells were then incubated in 10% horse serum, 0.1% Triton X-100/PBS for 30 min to minimize nonspecific antibody binding. The cells were incubated overnight with primary antibodies at 4 °C. The cell were washed with PBS four times and then incubated with the appropriate second antibody. The following primary antibodies were used: rabbit polyclonal antibodies: anti-ankyrin-G (0.8 μ g/ml) and anti- β 2-spectrin (0.5 μ g/ml); mouse monoclonal antibodies: anti-E-cadherin (2 μ g/ml; BD Biosciences), anti- α -Na/K-ATPase (4 μ g/ml; Affinity Bioreagents), anti- β -tubulin (1 μ g/ml; Santa Cruz Biotechnology), and ZO-1 (2 μ g/ml; Zymed Laboratories Inc.); goat polyclonal antibodies: anti- β -catenin (2 μ g/ml; Santa Cruz Biotechnology), anti-Ezrin (1 μ g/ml; Santa Cruz Biotechnology), and anti-Thy-1 (2 μ g/ml; Santa Cruz Biotechnology); pig polyclonal antibody: anti-GFP (1 μ g/ml). The secondary antibodies were all raised in donkey and included anti-mouse FITC, anti-mouse TRITC, anti-rabbit TRITC, anti-rabbit Cy5, anti-goat-FITC, and anti-swine FITC. Images were collected on a Zeiss LSM510 meta confocal microscope using either a 20 \times objective N.A 0.5 or 40 \times water immersion objective NA 1.2 and 1 \times digital zoom. A 100 \times oil objective NA 1.45 was used with a 1.4 \times digital zoom for observing cells undergoing cell division. Z stacks were collected at Z increments of 0.2 μ m. XZ images were obtained from Z stacks using the orthogonal function of the LSM510 software.

Immunoblot Analysis—SDS-PAGE and immunoblot analysis were performed as described (26). Anti-ankyrin-G C-terminal antibody was used at 0.8 μ g/ml. The primary antibody was detected using ¹²⁵I-protein A/G. The blot was exposed to a phosphor screen for 8 h, and the screen was scanned on a Typhoon 9200 variable mode imager.

RESULTS

Ankyrin-G Polypeptides Are Associated with the Lateral Membrane of Human Bronchial Epithelial Cells—This study

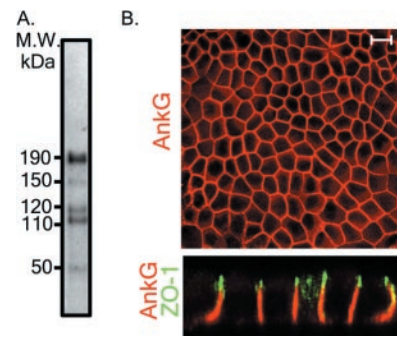


FIG. 1. Ankyrin-G (*AnkG*) polypeptides localize to the lateral membrane of human bronchial epithelial cells. *A*, immunoblot analysis using an affinity-purified antibody against the C-terminal regulatory domain of ankyrin-G reveals five cross-reacting polypeptides 190, 150, 120, 110, and 50 kDa in cells cultured for 26 h. *M.W.*, molecular weight. *B*, confocal immunofluorescence analysis on cells after 26 h in culture shows that ankyrin-G (red in XY and XZ sections) is polarized and localizes to the lateral membrane. ZO-1 (green) is a marker for tight junction in the XZ section. Scale bar, 20 μ m.

addresses the role of 190-kDa ankyrin-G in the formation of membrane domains in epithelial cells using the human bronchial epithelial cell line 16HBE14o– (27) as a model system. Although this cell line has been used primarily to study the physiology of human airway epithelium, it has several features useful in the study of epithelial cell domains. The cell line shows the presence of tight junctions and displays asymmetric distribution of proteins, and monolayers of the cell line generate transepithelial resistance (27, 28). In addition, these cells are of human origin, are morphologically uniform, and are readily transfected.

Immunoblot analysis of cell lysates from cells cultured for 26 h (see below) with affinity-purified antibody against the C-terminal regulatory domain of ankyrin-G revealed five ankyrin-G polypeptides of apparent molecular masses of 190, 150, 120, 110, and 50 kDa (Fig. 1*A*). XY and XZ confocal sections of cells following immunofluorescence analysis (Fig. 1*B*) show that ankyrin-G immunoreactive polypeptides localize to the lateral membrane below the tight junctions marked by ZO-1 staining (green). This pattern is in agreement with the recently reported (11, 12) localization of ankyrin-G to the lateral membrane in MDCK cells. It is unclear from our experiments which of the ankyrin-G polypeptides localize to the lateral membrane.

In some cells shown in the XZ confocal section, ZO-1 showed apicolateral staining (yellow in XZ section). Internal punctate localization of ZO-1 was observed in one cell. Such ZO-1 localization has been observed during the development of the tight junction both in cell culture as well as *in vivo* (29, 30).

Loss of the Lateral Membrane Following Depletion of 190-kDa Ankyrin-G—The pSuper plasmid (25) was used to drive the cellular expression of human 190-kDa ankyrin-G-specific small interfering RNA. The 19-nucleotide target sequences for the siRNA from homologous regions of the human and rat 190-kDa ankyrin-G are shown in Fig. 2*A*. The 19-nucleotide human target sequence for the human 190-kDa-specific siRNA differs from the homologous rat sequence (*, Fig. 2*A*) at three wobble positions. An siRNA that is different from the target nucleotide sequence at three positions is ineffective in producing knockdown (25). We have used the rat 190-kDa ankyrin-G-specific siRNA as an experimental control to monitor the nonspecific effects of expressing the human 190-kDa-specific siRNA in cells in all the following experiments. Plasmids directing expression of siRNA targeting human and rat 190-kDa ankyrin-G are designated pSuper-human-ankyrin-G and pSuper-rat-ankyrin-G, respectively.

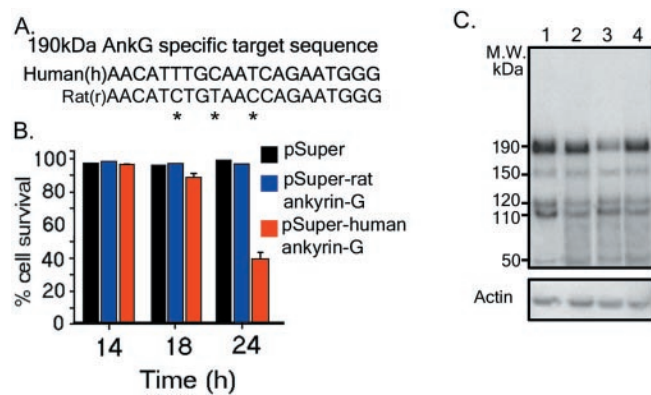


FIG. 2. Specific knockdown of 190-kDa ankyrin-G in human bronchial epithelial cells is achieved by transfecting the cells with a plasmid that directs the synthesis of an siRNA targeting 190-kDa ankyrin-G. A, the 19-nucleotide sequence with flanking 5' AA on the mRNA encoding the human 190-kDa ankyrin-G (*h*, top) and the rat 190-kDa ankyrin-G (*r*, bottom) that is targeted by the siRNA. * indicates the wobble position bases that are different in human and rat nucleotide sequences. The 19-nucleotide target sequence separated by a short spacer that forms a reverse complement of itself is cloned into the pSuper plasmid. This new plasmid encodes a transcript that serves as a precursor for the 190-kDa ankyrin-G-specific siRNA. Plasmids directing expression of siRNA targeting the human and the rat 190-kDa ankyrin-G are designated *pSuper-human-ankyrin-G* and *pSuper-rat-ankyrin-G*, respectively. B, cell survival as determined by trypan blue dye exclusion assay after transfection of cells with pSuper plasmids encoding 190-kDa ankyrin-G-specific siRNA. *x* axis represent times post-transfection when cells were tested for viability. *y* axis represents percentage of total cells on the dish that excluded the dye. The data represent the average of three independent experiments. Cells were transfected with pSuper (black bars), pSuper-rat-ankyrin-G (blue bars), and pSuper-human-ankyrin-G (red bars). C, the human siRNA depletes the 190-kDa ankyrin-G polypeptide and not the 150-, 120-, 110-, and 50-kDa ankyrin-G polypeptides. Immunoblot analysis of cells lysed 14 h after transfection with the following: no plasmid, lane 1; pSuper, lane 2; pSuper-human-ankyrin-G, lane 3; and pSuper-rat-ankyrin-G, lane 4. The rat siRNA sequence that varies from the human target sequence (* in A) is incapable of knocking down the 190-kDa ankyrin-G polypeptide and serves as a control for nucleotide sequence specificity of the siRNA. Upper panel, ankyrin-G immunoblot; lower panel, actin immunoblot.

The effect of pSuper plasmid-driven expression of the human 190-kDa-specific siRNA on cell viability was tested using a trypan blue dye exclusion assay (Fig. 2B). Cells were transfected with pSuper-human-ankyrin-G, pSuper-rat-ankyrin-G, and pSuper 12 h after plating, and post-transfection cell viability was tested. 40–60% of the cells were transfected, as judged by reduction in intensity of ankyrin-G immunofluorescence staining (see below). Only 40% of the cells were viable 24 h post-transfection with pSuper-human-ankyrin-G (red bar, Fig. 2B), in contrast to the 98% viability of cells transfected with pSuper (black bar, Fig. 2B), and pSuper-rat-ankyrin-G (blue bar, Fig. 2B). However, 98% of the cells transfected with pSuper-human-ankyrin-G survive 14 h after transfection. At the 14-h time point following transfection, cells have been in culture for 26 h and thus are the same as the cells in Fig. 1B. All the following experiments were performed 14 h post-transfection of cells, when cell viability is preserved.

Specific knockdown of 190-kDa ankyrin-G compared with the 150-, 120-, 110-, and 50-kDa ankyrin-G polypeptides was observed by immunoblot analysis of cell lysates from pSuper-human-ankyrin-G-transfected cells (lane 3, Fig. 2C). 190-kDa ankyrin-G is reduced by 40% in cell lysates from cells transfected with pSuper-human-ankyrin-G (lane 3, Fig. 2C) in comparison to cell lysates from untransfected (lane 1, Fig. 2C) and pSuper transfected (lane 2, Fig. 2C) cells. In contrast, the cell lysate from pSuper-rat-ankyrin-G plasmid-transfected cells showed levels of 190-kDa ankyrin-G polypeptide similar to that

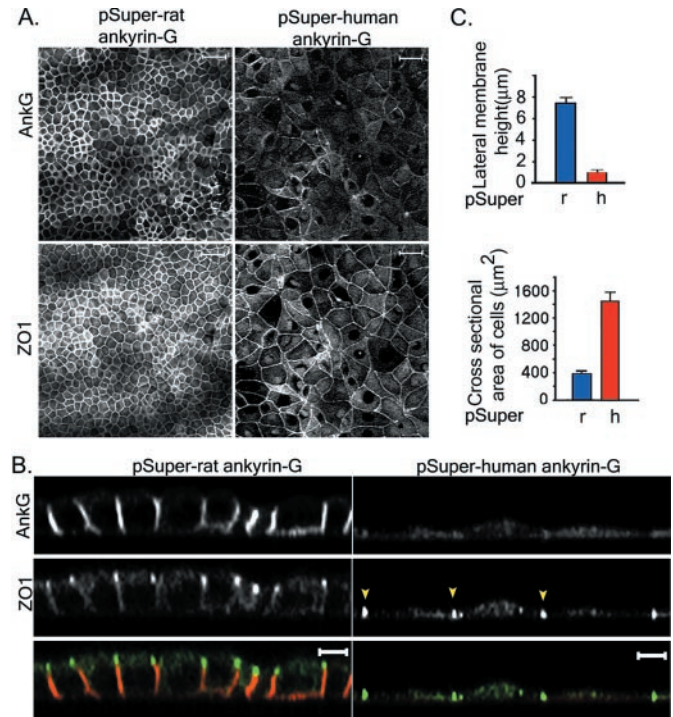


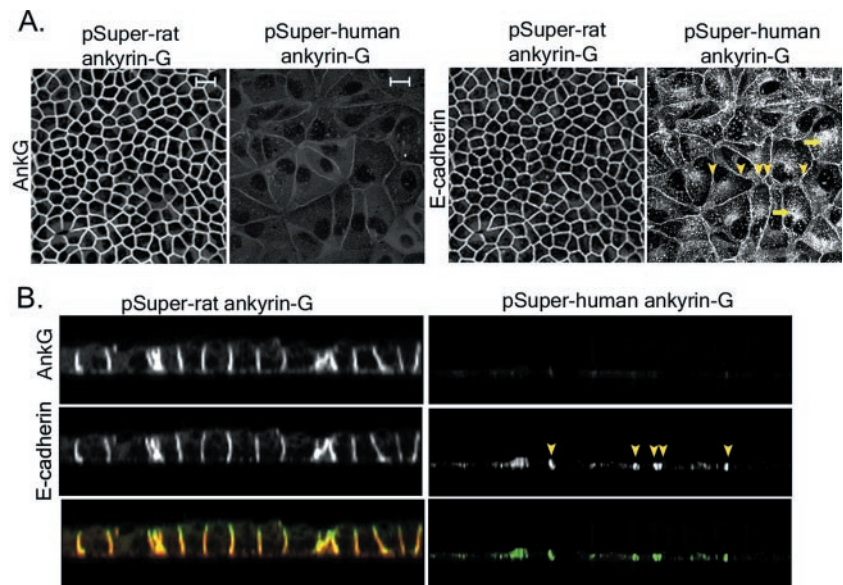
FIG. 3. Depletion of the 190-kDa ankyrin-G results in the loss of the lateral membrane in human bronchial epithelial cells. A, confocal microscopy shows that 190-kDa ankyrin-G knockdown results in increased cross-sectional area of cells without loss of cell-cell contact. XY confocal sections of cells were transfected with the plasmid pSuper-rat-ankyrin-G (left) that produces the rat 190-kDa ankyrin-G-specific siRNA or the pSuper-human-ankyrin-G plasmid (right) that codes for the human 190-kDa ankyrin-G-specific siRNA, then fixed, and stained with the antibodies anti-ankyrin-G (*AnkG*) (top) anti-ZO-1 (*ZO1*) (bottom). Scale, 50 μm . B, XZ confocal sections show loss of the lateral membrane but maintenance of tight junctions between cells as indicated by the localization of the tight junction protein ZO-1 after 190-kDa ankyrin-G knockdown in the cells. Cells were transfected with pSuper-rat-ankyrin-G (left) or pSuper-human-ankyrin-G (right) and then fixed and stained with anti-ankyrin-G (top, red channel in gray scale) and anti-ZO-1 (middle, green channel in gray scale). The image representing the merged ankyrin-G and ZO-1 immunofluorescence signals are shown at the bottom. Arrowheads point to sites of cell-cell contact labeled with ZO-1 that prevail after knockdown of 190-kDa ankyrin-G. Scale, 20 μm . C, bar graph (top) shows the loss of cell height, and bar graph (bottom) shows the increase in cross-sectional area of the cells after 190-kDa ankyrin-G knockdown. Cells were transfected with pSuper-human-ankyrin-G (*h*, red bar) and pSuper-rat-ankyrin-G (*r*, blue bar).

observed in cell lysates from untransfected (lane 1, Fig. 2C) and pSuper-transfected (lane 2, Fig. 2C) cells, indicating the lack of siRNA knockdown (lane 4, Fig. 2C). The comparable levels of ankyrin-G polypeptides different from the 190-kDa polypeptide in all four lanes show that a similar amount of total protein was present in each lane. This point is reinforced by the similar levels of actin in the four lanes.

The level of ankyrin-G at the plasma membrane, as determined by immunofluorescence, was reduced by an average of 80% in cells transfected with pSuper-human-ankyrin-G, in contrast to cells transfected with the control plasmid pSuper-rat-ankyrin-G. This indicates a large fraction of plasma membrane-associated ankyrin-G is the 190-kDa ankyrin-G polypeptide.

Depletion of 190-kDa ankyrin-G in bronchial epithelial cells resulted in the loss of the lateral membrane and expansion of apical and basal membranes (Fig. 3). The lateral membrane in control cells, seen extending from the tight junction marked by the ZO-1 staining to the base of the cell in the XZ section (left, Fig. 3B), is on the average of 7.3 μm in length (blue bar, top, Fig. 3C). In contrast, cells transfected with pSuper-human-

FIG. 4. E-cadherin is present at the adherens junction following loss of the lateral membrane in 190-kDa ankyrin-G-depleted human bronchial epithelial cells. Cells were transfected with pSuper-rat-ankyrin-G and pSuper-human-ankyrin-G (indicated on top of the panels). Transfected cells were stained with anti-ankyrin-G (*AnkG*) and E-cadherin (A and B). XY confocal sections of the cells are shown in A. XZ section of cells shown in A. B, the antibody used is indicated at the side of the panels. Arrowheads point to E-cadherin at sites of cell-cell contact in cells depleted of the 190-kDa ankyrin-G in A and B. 190-kDa ankyrin-G knockdown in cells also results in the intracellular accumulation of E-cadherin (A, arrows). Scale bar, 20 μ m.



ankyrin-G show an average length of lateral membrane of only 1 μ m (red bar, top, Fig. 3C). Decrease in lateral membrane length following 190-kDa ankyrin-G knockdown is accompanied by an increase in cross-sectional area compared with control cells. Cells depleted of 190-kDa ankyrin-G polypeptide are 3.2-fold larger in cross-sectional area (red bar, bottom, Fig. 3C) than control cells (blue bar, bottom, Fig. 3C).

Apical-Basal Cell Polarity Is Preserved Following the Loss of the Lateral Membrane in 190-kDa Ankyrin-G-depleted Cells—Both the XY (right, Fig. 3A) and XZ confocal sections (right, Fig. 3B) reveal that ZO-1 is retained at the plasma membrane between adjacent cells following the depletion of 190-kDa ankyrin-G. The arrowheads point to the sites of cell-cell contact where ZO-1 is still retained following 190-kDa ankyrin-G knockdown, despite the loss of the lateral membrane. Tight junctions therefore are preserved following depletion of 190-kDa ankyrin-G.

The adherens junction protein E-cadherin still localizes to the sites of cell-cell contact in cells depleted of the 190-kDa ankyrin-G (Fig. 4). Cells transfected with pSuper-human-ankyrin-G that show loss of 190-kDa ankyrin-G (left, Fig. 4A) retain E-cadherin (right, Fig. 4A) at the plasma membrane between adjacent cells as visualized in XY sections as well as XZ sections (arrowheads, Fig. 4B). In control cells, E-cadherin localizes with ankyrin-G at the lateral membrane, although ankyrin-G is not present at the tight junctions (Fig. 4, A and B). The loss of the 190-kDa ankyrin-G and the consequent loss of the lateral membrane are also accompanied by the intracellular accumulation of E-cadherin (arrows, Fig. 4A). Another adherens junction resident protein β -catenin was also retained at the plasma membrane between cells depleted of the 190-kDa ankyrin-G (Supplemental Material Fig. 1). β -Catenin, like E-cadherin, showed intracellular accumulation in 190-kDa ankyrin-G-depleted cells (Supplemental Material Fig. 1).

We next tested if the asymmetric distribution of proteins between the apical and basolateral membrane domains is maintained in cells depleted of 190-kDa ankyrin-G. XZ confocal sections of control cells show that α -Na/K-ATPase localized to the lateral membrane (NKA, left, Fig. 5A), whereas Thy-1 localized exclusively to the apical membrane (left, Fig. 5B). In cells depleted of the 190-kDa ankyrin-G, Thy-1 still was restricted to the apical surface (right, Fig. 5B). In addition, α -Na/K-ATPase that is lost from the plasma membrane following knockdown of 190-kDa ankyrin-G did not mislocalize to the apical membrane (left, Fig. 5B). β -2-Spectrin is also lost from

the plasma membrane following the depletion of 190-kDa ankyrin-G (see below, Fig. 6). Retention of the polarized distribution of proteins to the apical domain and preservation of adherens junction proteins at sites of cell-cell contact indicate that the apical-basal polarity is preserved in cells following depletion of the 190-kDa ankyrin-G.

Rat 190-kDa Ankyrin-G cDNA Prevents Loss of Lateral Membrane Due to Human Ankyrin-G siRNA—Rat 190-kDa ankyrin-G mRNA is predicted to be resistant to knockdown by the human 190-kDa ankyrin-G-specific siRNA because of the differences in sequence within the target site for the human-specific siRNA (Fig. 2) (25). Cells were transfected with a mixture of the pSuper-human-ankyrin-G plasmid and the plasmid bearing the cDNA encoding the rat 190-kDa ankyrin-G fused to GFP. The plasmid mixture contained a 10-fold excess of the pSuper-human-ankyrin-G plasmid over the rat ankyrin-G-GFP plasmid to ensure the knockdown of the endogenous human 190-kDa ankyrin-G in every cell that expressed the rat 190-kDa ankyrin-G-GFP. A GFP-specific affinity-purified antibody allowed detection of cells expressing the rat 190-kDa ankyrin-G-GFP. We used this strategy, as our ankyrin-G antibodies cannot distinguish human ankyrin-G from rat ankyrin-G. Rat 190-kDa ankyrin-G is resistant to knockdown by human 190-kDa-specific siRNA as predicted. Cells cotransfected with pSuper-human-ankyrin-G and the plasmid expressing rat 190-kDa ankyrin-G-GFP show expression of rat 190-kDa ankyrin-G-GFP protein at the plasma membrane similar to control cells cotransfected with pSuper and the rat 190-kDa ankyrin-G-GFP plasmid (bottom panels of 3rd column and 4th column, Fig. 6A).

Expression of rat 190-kDa ankyrin-G restored α -Na/K-ATPase and β -2-spectrin localization to the plasma membrane (top and middle panels, 3rd column, Fig. 6A) that was lost in cells cotransfected with pSuper-human ankyrin-G and GFP (top and middle panels, 2nd column). The increased cross-sectional area of cells resulting from depletion of the cellular 190-kDa ankyrin-G is also prevented by rat 190-kDa ankyrin-G (compare bottom panels, 2nd and 3rd columns). XZ confocal sections of cells cotransfected with the pSuper-human-ankyrin-G plasmid and the rat 190-kDa ankyrin-G-GFP plasmid show that exogenous rat 190-kDa ankyrin-G prevents the loss of the lateral membrane (right, Fig. 6B). In contrast, cells in the same XZ confocal section that do not express the rat 190-kDa ankyrin-G-GFP protein lack lateral membrane (right, Fig. 6B). GFP alone fails to preserve the lateral membrane in cells when coexpressed with human 190-kDa ankyrin-G-spe-

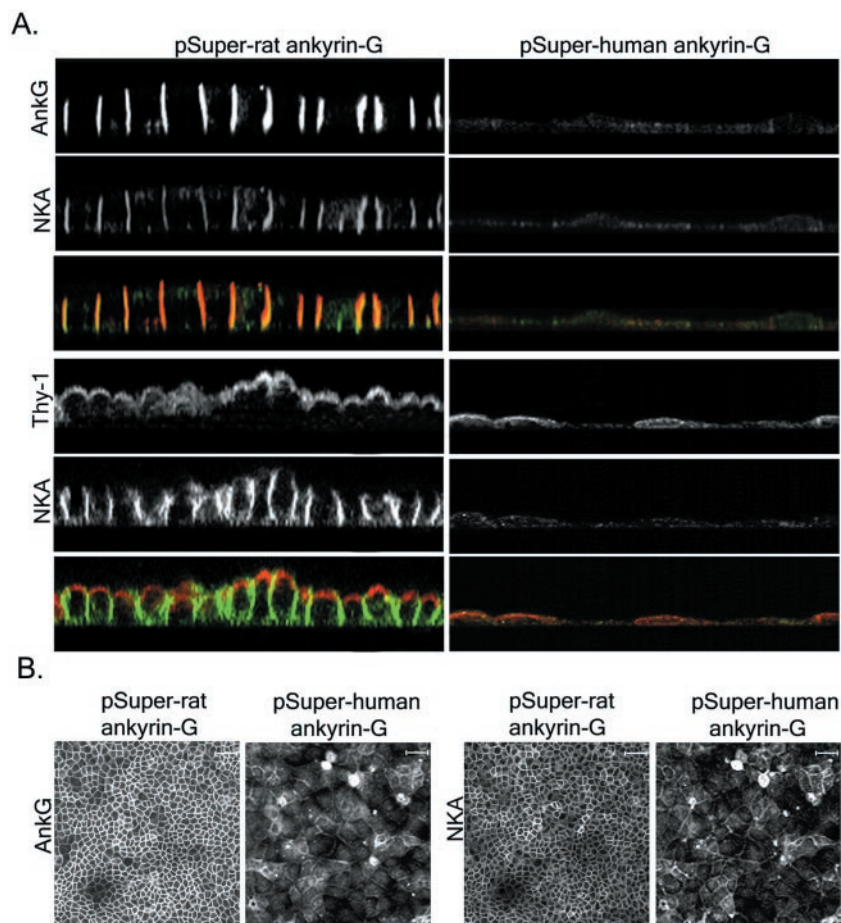


FIG. 5. The apical membrane polarity is preserved in human bronchial epithelial cells that have lost the lateral membrane as a result of 190-kDa ankyrin-G knockdown. A, XZ confocal sections of cells that have been transfected with pSuper-rat-ankyrin-G (*left*), pSuper-human-ankyrin-G (*right*), then fixed, and stained with anti-ankyrin-G (*top*, red channel in gray scale) and anti- α -Na/K-ATPase (*NKA*, middle, green channel in gray scale), an ankyrin-binding lateral membrane resident protein. *Bottom panels* represent a merge of ankyrin-G and α -Na/K-ATPase immunofluorescence signals. Ankyrin-G knockdown results in loss of lateral membrane plasma membrane as seen by the loss of α -Na/K-ATPase staining (compare *middle panels left and right*). B, siRNA knockdown of 190-kDa ankyrin-G results in an expanded apical membrane domain without compromising cell polarity. Cells transfected with pSuper plasmids expressing siRNA as in A were fixed and stained with antibodies against Thy-1 (*top*), an apical membrane resident glycosylinositol phosphate-linked protein, and α -Na/K-ATPase (*middle*, green channel in grayscale) a lateral membrane protein. A merged image of the Thy-1 α -Na/K-ATPase staining patterns is shown at the *bottom*. Loss of lateral membrane results in an expanded apical membrane (*right*) as visualized by Thy-1 (*top*) staining (compare Thy-1 staining in *left and right panels*). Note Thy-1 is still restricted to the apical surface in cell lacking the lateral membrane, and there is no α -Na/K-ATPase staining on the apical membrane indicating preservation of apical membrane polarity. C, XY confocal sections of cells transfected with pSuper plasmid expressing siRNA (indicated on *top of panels*) were fixed and stained with anti-ankyrin-G (*left*) and anti- α -Na/K-ATPase (*right*). Scale bar, 50 μ m.

cific siRNA (*left*, Fig. 6B). The ability of rat 190-kDa ankyrin-G to prevent loss of lateral membrane when coexpressed with human 190-kDa-specific siRNA indicates that the rat 190-kDa ankyrin-G is functionally equivalent to the human bronchial epithelial cell 190-kDa ankyrin-G.

The closely related human 220-kDa ankyrin-B, in contrast to rat 190-kDa ankyrin-G, does not preserve lateral membrane upon coexpression with the human 190-kDa ankyrin-G-specific siRNA (Fig. 7). Cells were cotransfected with pSuper-human-ankyrin-G and plasmids encoding either rat 190-kDa ankyrin-G-GFP (*GGG*, Fig. 7) or human 220-kDa ankyrin-B-GFP (*BBB*, Fig. 7). Ankyrin-B-GFP is resistant to human 190-kDa ankyrin-G siRNA, as affirmed by the GFP staining (*BBB*, *GFP panel* in Fig. 7). siRNA knockdown of endogenous 190-kDa ankyrin-G in cells showing expression of 220-kDa ankyrin-B-GFP still results in loss of α -Na/K-ATPase and β -2-spectrin from the plasma membrane and increase in cross-sectional area of the cells (*BBB*, *NKA*, and *spectrin panels* in Fig. 7). In contrast, the cells expressing the rat 190-kDa ankyrin-G-GFP (*GGG*, *NKA*, and *spectrin panels* in Fig. 7) still retain α -Na/K-ATPase and β -2-spectrin at the plasma membrane and have reduced cross-sectional area. These results indicate that 220-

kDa ankyrin-B-GFP is incapable of functionally replacing the endogenous human 190-kDa ankyrin-G.

190-kDa ankyrin-G contains three protein domains: the membrane-binding domain that interacts with membrane proteins, the spectrin-binding domain, and the death domain/C-terminal regulatory domain. GFP-tagged chimeric proteins composed of rat 190-kDa ankyrin-G and the human 220-kDa ankyrin-B protein domains have been used to probe the structure-function relationship of the 220-kDa ankyrin-B in ankyrin-B null neonatal cardiomyocytes (26). Chimeras were designated with a 3-letter code, where letters G and B indicate origin from ankyrin-G and ankyrin-B, respectively, and the first position indicates the origin of the membrane domain; the second position indicates the spectrin binding domain; and the third position indicates the C-terminal regulatory domain. XZ confocal sections of the cells reveal that the chimeras were expressed, as detected by the anti-GFP antibody staining (*GFP*, Fig. 7), and that none of the chimeras were able to prevent loss of the lateral membrane (*GGB*, *GBG*, *BGG*, *rescue plasmid*, Fig. 7). These results indicate that all three protein domains of 190-kDa ankyrin-G are critical for prevention of the loss of the lateral membrane. Given that ankyrins-B and -G have 60–70%

FIG. 6. Rat 190-kDa ankyrin-G is resistant to human 190-kDa ankyrin-G siRNA and prevents loss of the lateral membrane when expressed in human bronchial epithelial cells during siRNA depletion of endogenous 190-kDa ankyrin-G. *A* and *B*, coexpression of rat ankyrin-G-GFP (*rAnk-G-GFP*) but not GFP with pSuper-human-ankyrin-G plasmid encoding 190-kDa ankyrin-G-specific siRNA prevents the loss of lateral membrane and lateral membrane resident proteins β -2-spectrin and α -Na/K-ATPase (*NKA*). Cells were cotransfected with the pSuper-human-ankyrin-G (*h*) and rescue plasmids encoding GFP or rat ankyrin-G-GFP (listed above *top row of panels*) in a 10:1 ratio to ensure every cell expressing the rescue plasmid was depleted of 190 kDa of ankyrin-G. – indicates use of empty pSuper plasmid. 190-kDa rat ankyrin-G is resistant to the human 190-kDa ankyrin-G siRNA because of the variation in nucleotide sequence at three wobble positions (Fig. 2A). Cells were stained with three primary antibodies anti- β -2-spectrin (*top panels*), anti- α -Na/K-ATPase (*NKA*, *middle panels*), and anti-GFP (*bottom panels*). XY confocal sections are shown in *A* and XZ section in *B*. Scale, 50 μ m.

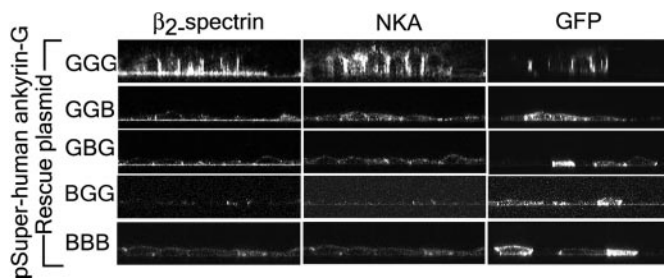
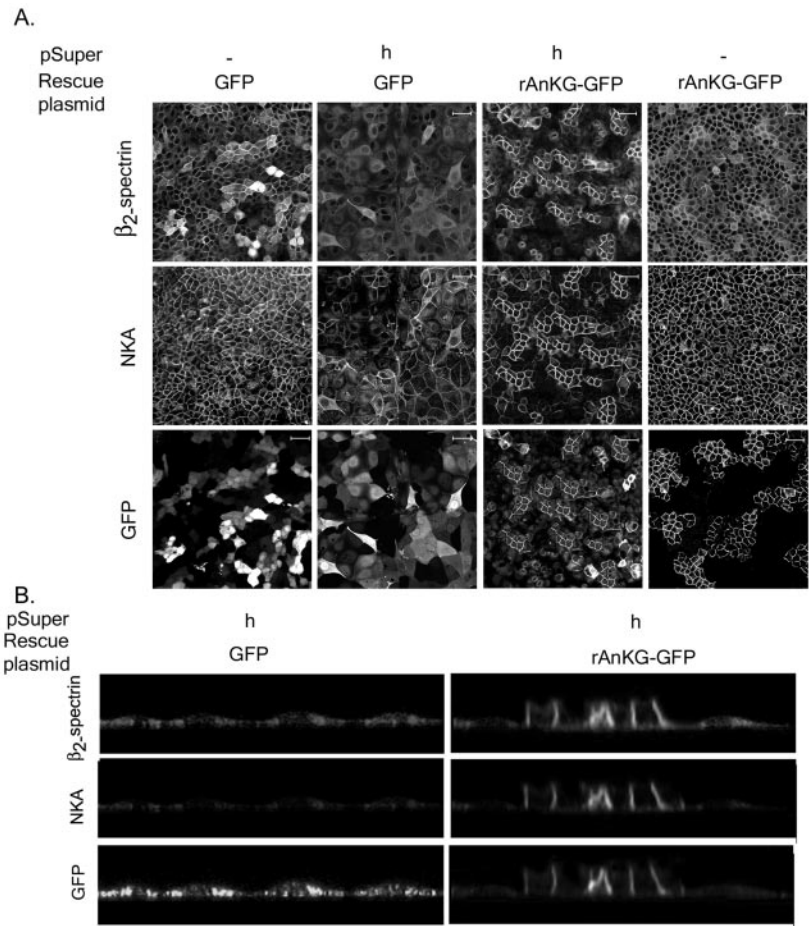


FIG. 7. Structure-function analysis using rat ankyrin-G and human ankyrin-B chimeras reveals that the ability to prevent loss of lateral membrane by expression during siRNA depletion of endogenous 190-kDa ankyrin-G is restricted to full-length 190-kDa ankyrin-G. XZ confocal sections of cells cotransfected with pSuper-human-ankyrin-G plasmid encoding the 190-kDa ankyrin-G-specific siRNA and rescue plasmids encoding rat 190-kDa ankyrin-G, human ankyrin-B, and chimeras of rat ankyrin-G and human ankyrin-B fused to GFP at the C terminus were stained with β -2-spectrin (*top panels*), α -Na/K-ATPase (*NKA*, *middle panels*), and anti-GFP (*bottom panels*). The composition of the chimeras is indicated by the three-letter code (G, ankyrin-G, and B, ankyrin-B) and is listed to the left of the panels. The letters at the three positions represent three major protein domains common to ankyrins. The *1st* letter represents the origin (ankyrin-G or ankyrin-B) of the membrane binding domain, the *2nd* letter the spectrin binding domain, and the *3rd* letter the death domain/C-terminal regulatory domain.

sequence identity in their membrane-binding and spectrin-binding domains, the capacity of only 190-kDa ankyrin-G to form the lateral membrane suggests a high level of specificity.

Depletion of 190-kDa Ankyrin-G Polypeptide Prevents Lateral Membrane Biogenesis during Cytokinesis—Loss of the lateral membrane following depletion of 190-kDa ankyrin-G could result from defective initial assembly and/or recycling or re-

modeling pathways. Polarized epithelial cells undergoing cell division create a new lateral membrane that separates the two daughter cells in the final phase of cytokinesis. For example, the lateral membrane in MDCKII cells undergoing cytokinesis is formed by the telophase stage and has a polarized distribution of E-cadherin (31). Mitotic cells thus provide a means of observing *de novo* biogenesis of the lateral membrane separate from secondary remodeling pathways.

We monitored formation of the lateral membrane between dividing human bronchial epithelial cells by observing the localization of marker proteins for the lateral membrane, ankyrin-G, β -2-spectrin, and β -catenin between late anaphase and late telophase stages of mitosis (Fig. 8). Formation of tight junctions was monitored by ZO-1 localization. The late anaphase stage of cell division was determined by formation of interzonal microtubules as revealed by localization of β -tubulin, and the late telophase stage was identified based on the presence of the midbody, again determined by β -tubulin localization (32). Fig. 8 shows both XY and XZ confocal images of cells in late anaphase and late telophase stages of cell division that have been stained with antibodies against β -tubulin (*green*) and antibody against one of the lateral membrane markers or ZO-1 (*red*). In late anaphase, the lateral membrane is a nub located at the base of dividing cells that stains intensely with the lateral membrane markers ankyrin-G, β -2-spectrin, and β -catenin (*arrow*, *anaphase*, Fig. 8). By late telophase the lateral membrane grows apically to the midbody (*arrow*, *telophase*, Fig. 8). ZO-1 (*red*) staining is granular in the cytoplasm of the dividing cell at late anaphase. However, by late telophase, ZO-1 staining has coalesced into an intense spot at the level of the midbody. These results indicate that the growth of the lateral membrane begins at late anaphase,

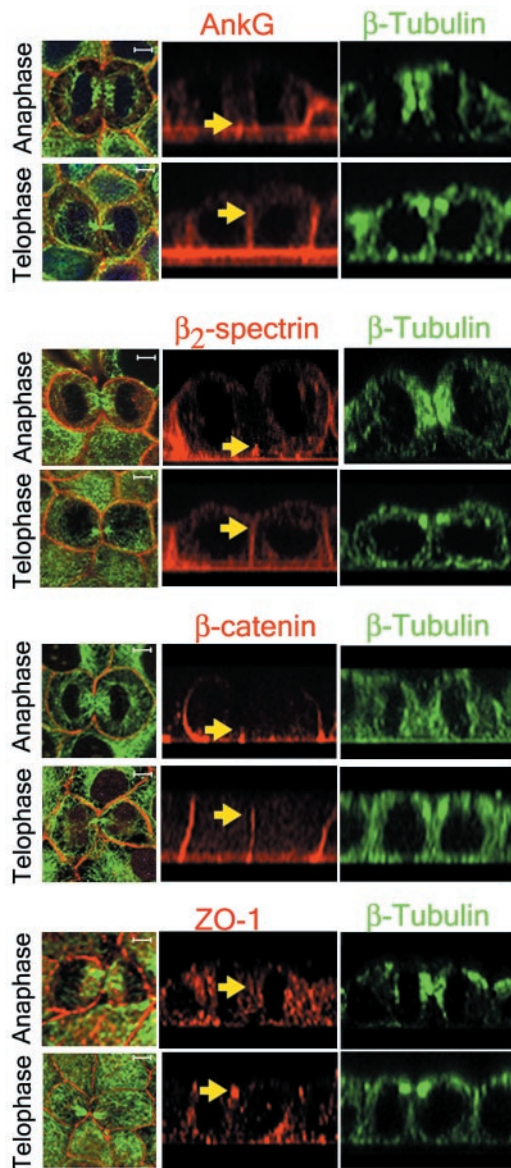


FIG. 8. Epithelial cells in a monolayer undergoing cytokinesis can be used as a model to study lateral membrane biogenesis. Dividing epithelial cells at late anaphase and late telophase that have been fixed and stained with β -tubulin (green) and four proteins ankyrin-G, β -2-spectrin, β -catenin, and ZO-1 (red) are shown in the four sets of panels. Each panel set consists of an XY confocal image of a dividing cell and an XZ image of the same cell. The XY images represent a merged image obtained from a double immunofluorescence labeling. The antibodies used are indicated above the panels. The XZ images representing ankyrin-G, β -2-spectrin, β -catenin, ZO-1 (red), and β -tubulin (green) are shown. The arrows point out the lateral membrane between the dividing cells at the anaphase and telophase stage. Ankyrin-G, β -2-spectrin, and β -catenin localize to the developing lateral membrane in contrast to ZO-1. Tubulin staining reveals the interzonal microtubules present at the late anaphase stage and the midbody structure in the late telophase stage. The lateral membrane that is restricted to the base of the cell in late anaphase increases in length and extends to the midbody structure by late telophase. Scale bar, 10 μ m.

progresses from the basal membrane to the apical tight junction, and displays an asymmetric distribution of proteins characteristic of a polarized epithelial cell lateral membrane (compare ZO1-localization with ankyrin-G localization) by late telophase.

We used the dividing cell model to determine whether 190-kDa ankyrin-G depletion affected *de novo* biogenesis of lateral membrane (Fig. 9). Cells transfected with pSuper-human-ankyrin-G to deplete cellular 190-kDa ankyrin-G were evalu-

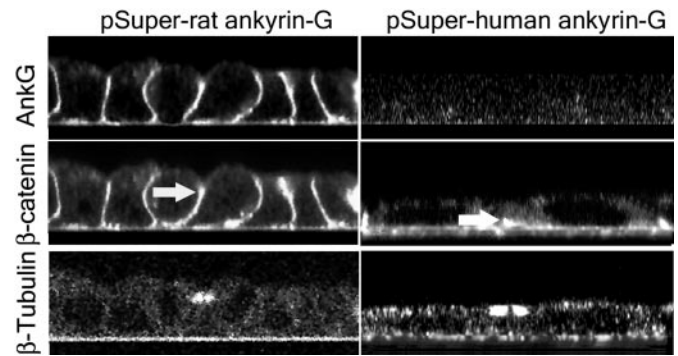


FIG. 9. 190-kDa ankyrin-G (*AnkG*) prevents lateral membrane biogenesis in epithelial cells undergoing cytokinesis. Cells that were transfected with pSuper-rat-ankyrin-G (left) or pSuper-human-ankyrin-G (right), fixed, and stained with top panels anti-ankyrin-G (red), anti- β -catenin (middle), and anti- β -tubulin (bottom). Cells in late telophase are shown. Arrow points to the developing lateral membrane between the dividing cells. Cell depleted of 190-kDa ankyrin-G fail (compare top panels) to extend the lateral membrane marked by β -catenin (compare middle panels) to the midbody structure.

ated for the ability to form a lateral membrane between the daughter cells during cytokinesis. As a control, cells were transfected with pSuper-rat-ankyrin-G. Cells in late telophase were identified by the presence of the midbody by localizing β -tubulin (bottom panel, Fig. 9). Cells that were transfected with pSuper-rat-ankyrin-G showed a well defined lateral membrane revealed by ankyrin-G and β -catenin localization that terminated below the midbody (top and arrow, middle, pSuper-rat, Fig. 9). 190-kDa ankyrin-G knockdown in pSuper-human-ankyrin-G transfected cells was determined by loss of anti-ankyrin-G staining (top, pSuper-human-ankyrin-G, Fig. 9). Cells depleted of 190-kDa ankyrin-G progress to late telophase stage as determined by formation of the midbody. β -Catenin was restricted to a nub (arrow, middle, pSuper-human, Fig. 9), reminiscent of lateral membrane seen at late anaphase in Fig. 8. These results demonstrate that knockdown of 190-kDa ankyrin-G prevents the growth of the lateral membrane, which arrests at the base of the cell. 190-kDa ankyrin-G therefore is required for lateral membrane biogenesis following cell division in bronchial epithelial cells.

The inability to complete cytokinesis due to lack of lateral membrane assembly could be a factor in loss of cell viability in 190-kDa ankyrin-G-depleted cells (Fig. 2). 14 h after transfection of cells with pSuper-human-ankyrin-G, 15% of the cells were binucleate in comparison to 2% in pSuper-rat-ankyrin-G transfected cells. By 24 h after transfection, 46% of the cells were binucleate in contrast to 3% of cells that were binucleate in pSuper-rat-ankyrin-G transfected cells. The presence of binucleate cells following depletion of 190-kDa ankyrin-G is consistent with incomplete cytokinesis due to failure in assembly of the lateral membrane.

DISCUSSION

This study demonstrates an unanticipated requirement of 190-kDa ankyrin-G for steady state accumulation of lateral membranes and in *de novo* biogenesis of lateral membrane following mitosis in bronchial epithelial cells. Depletion of 190-kDa ankyrin-G by small interfering RNA results in the nearly complete loss of the lateral plasma membrane in interphase cells. Loss of the lateral membrane domain is accompanied by an expansion of apical and basal plasma membranes and preservation of apical-basal polarity. Loss of lateral membrane can be prevented by cotransfection with rat 190-kDa ankyrin-G cDNA, which is resistant to human siRNA, but not by the closely related human 220-kDa ankyrin-B. These results suggest that the current paradigm for ankyrin function in coupling

the Na/K-ATPase to a preformed spectrin-actin network requires serious revision.

Loss of lateral membrane in 190-kDa ankyrin-G-depleted cells is balanced by an increase in surface area of apical and basal membranes. The overall synthesis of plasma membrane thus is preserved, suggesting normal function of ER and Golgi pathways in 190-kDa ankyrin-G-depleted cells. These results also indicate a separate, 190-kDa ankyrin-G-dependent pathway that is specifically required for assembly of the lateral membrane domain. The ankyrin-G dependent events responsible for lateral membrane domain formation are likely to occur in a post-Golgi compartment. Identification of the ankyrin-G compartment is an important challenge for future investigation.

These findings in epithelial cells suggests that 270/480-kDa ankyrin-G may similarly contribute to assembly of the excitable membrane domains of axon initial segments of neurons and nodes of Ranvier. These splice forms differ from 190-kDa ankyrin-G by insertion of sequence between the spectrin-binding and death/regulatory domain but otherwise are identical (7, 33). 270/480-kDa ankyrin-G clusters define both the initial segment and the nodes of Ranvier early in development (8, 34). β IV spectrin also accumulates at these developing initial segments (8, 35, 36), although clustering of β IV spectrin does not occur in the absence of ankyrin-G (8). The voltage-gated sodium channel Nav1.6 and the L1 cell adhesion molecule neurofascin are recruited only after formation of ankyrin-G clusters on the developing axon initial segments and node of Ranvier (8, 34). Moreover, depletion of cerebellar ankyrin-G results in loss of β IV spectrin and voltage-gated sodium channel from the axon initial segment (8) in a manner similar to the loss of β -2-spectrin and Na/K-ATPase in 190-kDa ankyrin-G-depleted epithelial cells.

190-kDa ankyrin-G is the first protein that we are aware of that has been shown to be required for the biogenesis of the lateral membrane in a mammalian polarized epithelial cell. Previous studies resulting in identification of proteins involved in lateral membrane domain formation have resulted from analysis of *Drosophila* mutants. Scribble, lethal giant larvae, and discs-large are three *Drosophila* proteins that have been implicated in the formation of the lateral membrane domain during early phases of *Drosophila* embryonic development (37, 38). However, these proteins are not essential for development of the lateral membrane, because cells lacking them recover to form polarized epithelial cells in late embryogenesis (38). These results indicate an unidentified pathway is required for formation of the lateral membrane. Our findings raise the possibility that this unidentified mechanism of lateral membrane biogenesis may involve 190-kDa ankyrin-G.

Adaptor complexes AP1-B and AP-4 have been implicated in trafficking of specific proteins selected based on targeting motifs to the basolateral membrane in mammalian epithelial cells (39, 40). Depletion of the μ 4 subunit of the AP4 complex results in loss of basolateral targeting of certain membrane proteins, although global loss of the basolateral membrane domain was not reported (39, 40). The ankyrin-G-dependent accumulation of lateral membrane presumably involves phospholipids as well as proteins and, in contrast to clathrin adaptors, seems unlikely to be coded by simple targeting motifs.

The mammalian homologue of the yeast exocyst complex sec6/8 has been implicated in targeting of membrane proteins to the basolateral domain using antibody inhibition of sec8 in streptolysin O-permeabilized MDCK cells (41). Moreover, overexpression of sec10 promotes formation of lateral membrane in MDCK cells, leading to taller cells (42). The effect of depleting sec6/8 on the integrity of the lateral membrane has not been

reported in tissue culture. However, it has been demonstrated recently (43) that transgenic siRNA depletion of *Drosophila* sec10, the most conserved protein component of the sec6/8 complex, does not affect epithelial cell polarity. These considerations suggest that ankyrin-G may not act through the exocyst-based targeting pathway.

It will be of interest to determine whether ankyrin-G functionally interacts with any of the mammalian homologues of *Drosophila* proteins implicated in lateral membrane formation, such as lethal giant larvae and discs large (44, 45). Lethal giant larvae has been shown to interact with syntaxin-4, the target-soluble NSF attachment protein receptors residing in the lateral membrane of epithelial cells (44). Cold-sensitive alleles of the yeast homologues of lethal giant larvae show accumulation of post-Golgi exocytic vesicles under nonpermissive temperatures (46). It is also possible that ankyrin-G accomplishes its function in lateral membrane biogenesis through an as yet unidentified pathway.

We have found that ankyrin-G localizes to the basolateral membrane of trophectoderm cells in the blastocyst, which are the first polarized epithelial cells in the developing embryo.² This early expression combined with the finding that ankyrin-G-depleted cells cannot complete cytokinesis suggests that null alleles of ankyrin-G gene will result in lethality. Thus, the role of ankyrin-G in lateral membrane biogenesis would not have been discovered without the cell culture model and siRNA depletion of ankyrin-G. This system can be used to study the function of other genes that are essential and expressed at an early embryonic stage.

Acknowledgments—Peter Mohler is gratefully acknowledged for sharing ankyrin-G and -B cDNAs and for the suggestion of using human bronchial epithelial cells. Lydia Davis is gratefully acknowledged for preparation of affinity-purified antibodies against ankyrin-G, GFP, and β -2-spectrin.

REFERENCES

- Lecuit, T., and Pilot, F. (2003) *Nat. Cell Biol.* **5**, 103–108
- Mostov, K., Su, T., and ter Beest, M. (2003) *Nat. Cell Biol.* **5**, 287–293
- Knust, E., and Bossinger, O. (2002) *Science* **298**, 1955–1959
- Tepass, U., Tanentzapf, G., Ward, R., and Fehon, R. (2001) *Annu. Rev. Genet.* **35**, 747–784
- Wodarz, A. (2002) *Nat. Cell Biol.* **4**, E39–E44
- Bennett, V., and Baines, A. J. (2001) *Physiol. Rev.* **81**, 1353–1392
- Kordeli, E., Lambert, S., and Bennett, V. (1995) *J. Biol. Chem.* **270**, 2352–2359
- Jenkins, S. M., and Bennett, V. (2001) *J. Cell Biol.* **155**, 739–746
- Zhou, D., Lambert, S., Malen, P. L., Carpenter, S., Boland, L. M., and Bennett, V. (1998) *J. Cell Biol.* **143**, 1295–1304
- Nelson, W. J., and Veshnock, P. J. (1987) *Nature* **328**, 533–536
- Thevananthar, S., Kolli, A. H., and Devarajan, P. (1998) *J. Biol. Chem.* **273**, 23952–23958
- Woroniecki, R., Ferdinand, J. R., Morrow, J. S., and Devarajan, P. (2003) *Am. J. Physiol.* **284**, F358–F364
- Yeaman, C., Grindstaff, K. K., and Nelson, W. J. (1999) *Physiol. Rev.* **79**, 73–98
- McNeill, H., Ozawa, M., Kemler, R., and Nelson, W. J. (1990) *Cell* **62**, 309–316
- Pradhan, D., Lombardo, C. R., Roe, S., Rimm, D. L., and Morrow, J. S. (2001) *J. Biol. Chem.* **276**, 4175–4181
- Nelson, W. J., Shore, E. M., Wang, A. Z., and Hammerton, R. W. (1990) *J. Cell Biol.* **110**, 349–357
- Devarajan, P., Stabach, P. R., De Matteis, M. A., and Morrow, J. S. (1997) *Proc. Natl. Acad. Sci. U. S. A.* **94**, 10711–10716
- Moorthy, S., Chen, L., and Bennett, V. (2000) *J. Cell Biol.* **149**, 915–930
- Norman, K. R., and Moerman, D. G. (2002) *J. Cell Biol.* **157**, 665–677
- Hammarlund, M., Davis, W. S., and Jorgensen, E. M. (2000) *J. Cell Biol.* **149**, 931–942
- Hu, R. J., Moorthy, S., and Bennett, V. (1995) *J. Cell Biol.* **128**, 1069–1080
- Huotari, V., Vaaranemi, J., Lehto, V. P., and Eskelinen, S. (1996) *J. Cell Physiol.* **167**, 121–130
- Otsuka, A. J., Franco, R., Yang, B., Shim, K. H., Tang, L. Z., Zhang, Y. Y., Boontrakulpoontawee, P., Jeyaparakash, A., Hedgecock, E., and Wheaton, V. I. (1995) *J. Cell Biol.* **129**, 1081–1092
- Otsuka, A. J., Boontrakulpoontawee, P., Rebeiz, N., Domanus, M., Otsuka, D., Velamparampill, N., Chan, S., Vande Wyngaerde, M., Campagna, S., and Cox, A. (2002) *J. Neurobiol.* **50**, 333–349
- Brummelkamp, T. R., Bernards, R., and Agami, R. (2002) *Science* **296**, 550–553
- Mohler, P. J., Gramolini, A. O., and Bennett, V. (2002) *J. Biol. Chem.* **277**,

² K. Kizhatil and V. Bennett, unpublished data.

- 10599–10607
27. Cozens, A. L., Yezzi, M. J., Kunzelmann, K., Ohrui, T., Chin, L., Eng, K., Finkbeiner, W. E., Widdicombe, J. H., and Gruenert, D. C. (1994) *Am. J. Respir. Cell Mol. Biol.* **10**, 38–47
28. Mohler, P. J., Kreda, S. M., Boucher, R. C., Sudol, M., Stutts, M. J., and Milgram, S. L. (1999) *J. Cell Biol.* **147**, 879–890
29. Rajasekaran, A. K., Hojo, M., Huima, T., and Rodriguez-Boulau, E. (1996) *J. Cell Biol.* **132**, 451–463
30. Sheth, B., Fontaine, J. J., Ponzia, E., McCallum, A., Page, A., Citi, S., Louvard, D., Zahraoui, A., and Fleming, T. P. (2000) *Mech. Dev.* **97**, 93–104
31. Reinsch, S., and Karsenti, E. (1994) *J. Cell Biol.* **126**, 1509–1526
32. Straight, A. F., and Field, C. M. (2000) *Curr. Biol.* **10**, R760–770
33. Peters, L. L., John, K. M., Lu, F. M., Eicher, E. M., Higgins, A., Yialamas, M., Turtzo, L. C., Otsuka, A. J., and Lux, S. E. (1995) *J. Cell Biol.* **130**, 313–330
34. Jenkins, S. M., and Bennett, V. (2002) *Proc. Natl. Acad. Sci. U. S. A.* **99**, 2303–2308
35. Komada, M., and Soriano, P. (2002) *J. Cell Biol.* **156**, 337–348
36. Berghs, S., Aggujaro, D., Dirx, R., Jr., Maksimova, E., Stabach, P., Hermel, J. M., Zhang, J. P., Philbrick, W., Slepnev, V., Ort, T., and Solimena, M. (2000) *J. Cell Biol.* **151**, 985–1002
37. Muller, H. A. (2003) *Dev. Cell* **4**, 1–3
38. Tanentzapf, G., and Tepass, U. (2003) *Nat. Cell Biol.* **5**, 46–52
39. Simmen, T., Honing, S., Icking, A., Tikkanen, R., and Hunziker, W. (2002) *Nat. Cell Biol.* **4**, 154–159
40. Folsch, H., Ohno, H., Bonifacino, J. S., and Mellman, I. (1999) *Cell* **99**, 189–198
41. Grindstaff, K. K., Yeaman, C., Anandasabapathy, N., Hsu, S. C., Rodriguez-Boulau, E., Scheller, R. H., and Nelson, W. J. (1998) *Cell* **93**, 731–740
42. Lipschutz, J. H., Guo, W., O'Brien, L. E., Nguyen, Y. H., Novick, P., and Mostov, K. E. (2000) *Mol. Biol. Cell* **11**, 4259–4275
43. Andrews, H. K., Zhang, Y. Q., Trotta, N., and Broadie, K. (2002) *Traffic* **3**, 906–921
44. Musch, A., Cohen, D., Yeaman, C., Nelson, W. J., Rodriguez-Boulau, E., and Brennwald, P. J. (2002) *Mol. Biol. Cell* **13**, 158–168
45. Wu, H., Reuver, S. M., Kuhlendahl, S., Chung, W. J., and Garner, C. C. (1998) *J. Cell Sci.* **111**, 2365–2376
46. Lehman, K., Rossi, G., Adamo, J. E., and Brennwald, P. (1999) *J. Cell Biol.* **146**, 125–140 .